4

# Ferroelectric Properties and Polarization Switching Kinetic of Poly (vinylidene fluoride-trifluoroethylene) Copolymer

Duo Mao, Bruce E. Gnade and Manuel A. Quevedo-Lopez
*Department of Material Science and Engineering, The University of Texas at Dallas*
*USA*

## 1. Introduction

The discovery of the piezoelectric properties of poly(vinylidene fluoride) (PVDF) by Kawai [Kawai, 1969], and the study of its pyroelectric and nonlinear optical properties [Bergman et al., 1971; Glass, 1971] led to the discovery of its ferroelectric properties in the early 1970s. Since that time, considerable development and progress have been made on both materials and devices based on PVDF. This work helped establish the field of ferroelectric polymer science and engineering [Nalwa, 1995a]. There are many novel ferroelectric polymers, such as poly(vinylidene fluoride) (PVDF) copolymers, poly(vinylidene cyanide) copolymers, odd-numbered nylons, polyureas, ferroelectric liquid crystal polymers and polymer composites of organic and inorganic piezoelectric ceramics [Nalwa, 1991 and Kepler & Anderson, 1992 as cited in Nalwa, 1995b; Nalwa, 1995a]. Among them, PVDF, and its copolymers are the most developed and promising ferroelectric polymers because of their high spontaneous polarization and chemical stability.

Ferroelectricity is caused by the dipoles in crystalline or polycrystalline materials that spontaneously polarize and align with an external electric field. The polarization of the dipoles can be switched to the opposite direction with the reversal of the electric field. Similar to inorganic ferroelectric materials such as $PbZr_{0.5}Ti_{0.5}O_3$ (PZT) and $SrBi_2Ta_2O_9$ (SBT), organic ferroelectric materials exhibit ferroelectric characteristics such as Curie temperature (the transition temperature from ferroelectrics to paraelectrics), coercive field (the minimum electric field to reverse the spontaneous polarization) and remanent polarization (the restored polarization after removing the electric field). However, the low temperature and low fabrication cost of organic ferroelectric materials enable them to be used in a large number of applications, such as flexible electronics.

In this chapter, the discussion is focused on poly(vinylidene fluoride-trifluoroethylene) [P(VDF-TrFE)], one of the most promising PVDF ferroelectric copolymers. The main objective of this chapter is to describe the ferroelectric properties of P(VDF-TrFE) copolymer and review the current research status of ferroelectric devices based on this material. The chapter is divided in six sections. The first section introduces the topic of organic ferroelectrics. The second section describes the material properties of the ferroelectric phase of P(VDF-TrFE) including phase structures, surface morphology, crystallinity and molecule chain orientation. Next, the electrical properties such as polarization, switching current, etc.

are discussed. In section four, the fundamental ferroelectric polarization switching mechanisms are introduced and the models for P(VDF-TrFE) thin films are reviewed. The nucleation-limited-switching (NLS) model, based on region-to-region switching kinetics for P(VDF-TrFE) thin film will be emphasized. The fifth section reviews the impact of annealing temperature, film thickness and contact dependence for P(VDF-TrFE) based ferroelectric capacitors. Finally, the most important results from this chapter will be summarized, and one of the P(VDF-TrFE) copolymer's potential applications as flexible non-volatile ferroelectric random access memory will be briefly discussed.

## 2. Material properties of P (VDF-TrFE) copolymer

P(VDF-TrFE) is a random copolymer synthesized using two homopolymers, PVDF and poly(trifluoroethylene) (PTrFE). The chemical formula is shown in Figure 1. PVDF is a crystalline polymer, has a monomer unit of $-CH_2-CF_2-$, in between polyethylene (PE) ( $-CH_2-CH_2-$) and polytetrafluoroethylene (PTFE) ($-CF_2-CF_2-$) monomers. The similarity of PVDF to these two polymers gives rise to its physical strength, flexibility and chemical stability [Tashiro, 1995]. Its ferroelectric properties originate from the large difference in electronegativity between fluorine, carbon and hydrogen, which have Pauling's values of 4.0, 2.5 and 2.1, respectively [Pauling, 1960]. Most of the electrons are attracted to the fluorine side of the polymer chain and polarization is created [Salimi & Yousefi, 2004; Fujisaki et al., 2007]. The Curie temperature of PVDF is estimated to be above the melting temperature at 195-197 $^oC$ [Lovinger, 1986, as cited in Kepler, 1995]. The melting of the ferroelectric phase and recrystallization to the paraelectric phase may happen in the same temperature range. The addition of TrFE ($-CF_2-CFH-$) into the PVDF system plays an important role in the phase transition behavior. TrFE modifies the PVDF crystal structure by increasing the unit cell size and inter-planar distance of the ferroelectric phase, as seen from X-ray diffraction measurements [Tashiro et al., 1984; Lovinger et al.., 1983a, 1983b, as cited in Tashiro, 1995]. The interactions between each unit and between dipole-to-dipole are reduced, resulting in a lower Curie temperature. Therefore, it allows the copolymer to crystallize into the ferroelectric phase at temperatures below the melting point. The copolymer crystal structure, phase transition behavior and ferroelectric properties are affected by the ratio of VDF/TrFE content and the synthesizing conditions [Yamada & Kitayama, 1981]. The experimental data from UT Dallas shown in this chapter are for P(VDF-TrFE) copolymer with 70/30 (VDF/TrFE), synthesized using a suspension polymerization process. The ferroelectric properties are measured and tested at room temperature, except if stated otherwise.

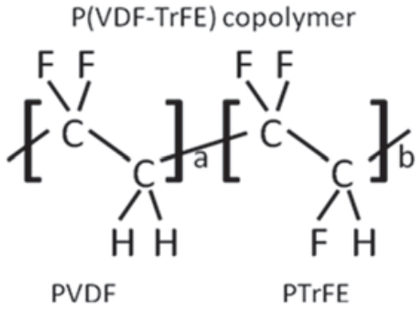


Fig. 1. The chemical formula of P(VDF-TrFE) random copolymer [Naber et al., 2005].

### 2.1 Phase structures

When the P(VDF-TrFE) copolymer chains are packed and form a solid material, there are four types of crystalline phases. The phase configurations are very similar to PVDF, including phase I (β), phase II (α), phase III (γ), and phase IV (δ) [Xu et al., 2000]. Among these four phases, only the β phase is the polar phase with a large spontaneous polarization along the b axis which is parallel to the C-F dipole moment, and perpendicular to the polymer chain direction (c axis) [Hu et al., 2009.]

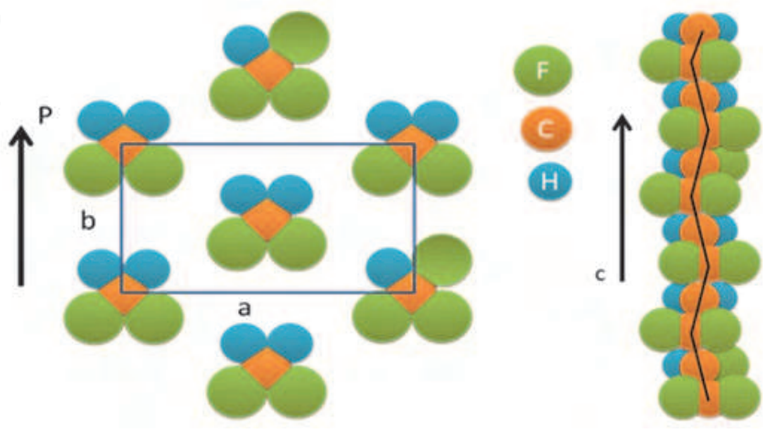


(a) (b)

Fig. 2. (a)The schematic of the β phase crystal structure for P(VDF-TrFE) copolymer in the ab plane (the c axis is normal to the ab plane), and (b) along the c axis of the all-trans (TTTT) zigzag planar configuration from the top view.

The schematic of the β phase crystal structure is shown in Figure 2. The molecules are in a distorted, all-trans (TTTT) zigzag planar configuration. When the polymer is cooled from its melt state, it crystallizes into the α phase. This crystal is nonpolar with the molecules in a distorted trans-gauche-trans-gauche' (TGTG') configuration, which is the state with the lowest energy. In the γ phase, the crystal has polar unit cells with molecules in the $T_3GT_3G'$ configuration, and the dipole moment is smaller than phase I (β). For the δ phase, the crystal has the same configuration as the α phase, but with a different orientation of the molecules' dipole moments in the unit cell [Kepler, 1995]. Different phases can be achieved by using different processing conditions. The material can transition between phases by using annealing, stretching and poling methods [Tashiro et al., 1981, as cited in Tashiro 1995]. In this chapter, the discussion is focused on the polar β phase.

### 2.2 Surface morphology of β phase crystals

The mechanics and aggregation characteristics of the polymeric chains can be different when forming each crystalline phases, resulting in different surface morphologies. This can be studied using atomic force microscopy (AFM). Figure 3 shows a 3D 1μm×1μm AFM image of a typical P(VDF-TrFE) film. The rod-like shape of the grains is attributed to the β phase crystallites. The size of the grains and the roughness of the surface are related to the annealing conditions and are sensitive to the maximum processing temperature [Park et al., 2006; Mao et al., 2010a]. The sample shown in Figure 3 corresponds to a 210 nm spin coated film annealed at 144 °C for 2 hours in vacuum. The length of the grains is approximately 180 nm with a surface RMS roughness of 14.6 nm [Mao et al., 2010a].

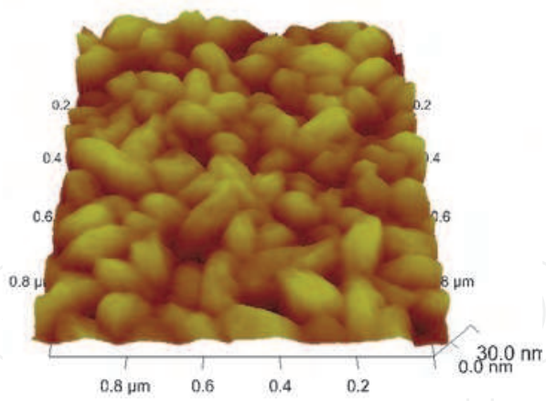


Fig. 3. AFM tapping mode height image of a 210 nm P(VDF-TrFE) film annealed at 144 °C for 2 hours in vacuum.

### 2.3 X-ray analysis for β phase crystals

X-ray Diffraction (XRD) can be used to study the crystalline characteristics. The diffraction angle corresponds to the inter-planar spacing and orientation of the crystal planes, and the diffraction intensity indicates the quantity of the corresponding crystal planes, which relates to the degree of crystallinity. The crystal structure of P(VDF-TrFE) is normally related to the composition (mole ratio of VDF/TrFE) of the copolymer and the annealing process. In the β crystal phase of P(VDF-TrFE), the unit cell is orthorhombic, with each chain aligned and packed with the $CF_2$ groups parallel to the b axis [Lando et al, 1966; Gal'perin & Kosmynin, 1969; Hasegawa et al, 1972, as cited in Tashiro, 1995], as indicated in Figure 2 (a). Figure 4 shows the XRD results from a 210 nm P(VDF-TrFE) (VDF/TrFE of 70/30) film annealed at 144 °C and measured at room temperature. The diffraction peak at $2\theta=19.9^{o}$ is attributed to the (110) and (200) orientation planes, which are associated with the polar β phase. From the position of this sharp peak, the inter-planar spacing b is determined to be 4.5 Å [Mao et al, 2010a]. The strong diffraction peak indicates a high degree of crystallinity in the β phase.

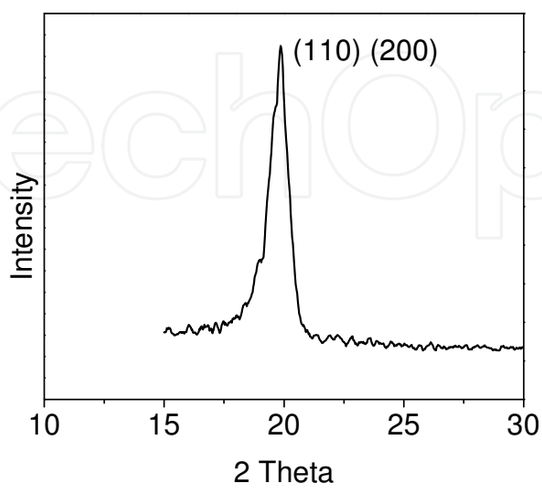


Fig. 4. XRD results for 210 nm β phase P(VDF-TrFE) (VDF/TrFE of 70/30) film annealed at 144 °C and measured at room temperature

### 2.4 Vibrational analysis for β phase crystals

Molecular vibration analysis is a key to understanding the dynamics of a material. Fourier-transform infrared spectroscopy (FT-IR) can be used to detect the vibrational mechanics of a material system by monitoring the absorption of infrared energy. The incident electro-magnetic field from the IR source interacts with the molecular bonding of the P(VDF-TrFE) film, resulting in a large absorption when the molecular vibration and the electric field component of the IR are perpendicular to each other. Each phase of the P(VDF-TrFE) polymer will provide a characteristic FT-IR spectrum. Details of the absorption band assignments can be found in the literature [Kobayashi et al, 1974; Reynolds et al, 1989; Kim et al, 1989]. Here we only discuss the three intense bands, 1288 $cm^{-1}$, 850 $cm^{-1}$, and 1400 $cm^{-1}$ associated with the β phase of P(VDF-TrFE). The 1288 $cm^{-1}$ and 850 $cm^{-1}$bands belong to the $CF_2$ symmetric stretching with the dipole moments parallel to the polar b axis [Reynolds et al, 1989]. The 1400 $cm^{-1}$ band is assigned to the $CH_2$ wagging vibration, with the dipole moment along the c axis. As illustrated in Figure 5 [Mao et al, 2010], a polarized IR source with the electrical component parallel to the substrate (p-polarized) is used to measure two P(VDF-TrFE) thin film samples. The strong absorption bands at 1288 $cm^{-1}$ and 850 $cm^{-1}$ in spectrum A (sample A) indicates that the polar b axis of the P(VDF-TrFE) copolymer chain is perpendicular to the substrate and the planar zigzag chains are aligned parallel to the substrate [Hu et al, 2009]. However, in spectrum B (sample B), week absorption bands observed at 1288 $cm^{-1}$ and 850 $cm^{-1}$ indicate that the b axis is tilted away from the direction normal to the substrate. Additionally, the strong absorption band at 1400 $cm^{-1}$ band indicates the polymer chain (c axis) is tilted, and a significant number of the molecules are aligned normal to the substrate, which is undesirable for vertical polarization [Park et al, 2006; Mao et al, 2010a].

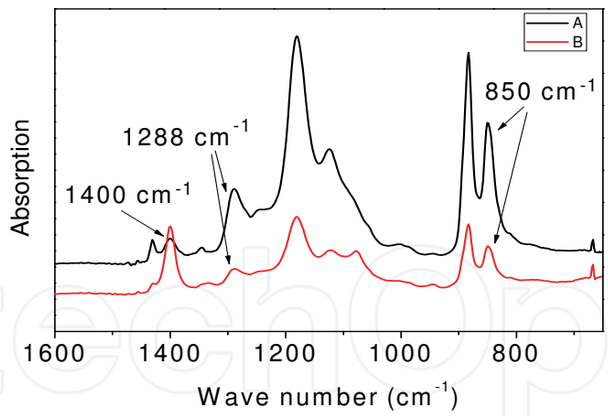


Fig. 5. FT-IR analysis of the β phase of P(VDF-TrFE) polymer films (A and B) with different polymer chain alignment characteristics. In sample A, the polymer chains are aligned parallel to the substrate, and in sample B, the polymer chains are tilted and some portions are aligned perpendicular to the substrate.

## 3. Electrical properties of P(VDF-TrFE) film

The fabrication of the polymer films into devices and the electrical characterization of the ferroelectric properties are introduced here. The discussion focuses on ferroelectric capacitors (FeCap), which is the fundamental device for studying this material.

### 3.1 Deposition of P(VDF-TrFE) films

There are two common methods to prepare P(VDF-TrFE) thin films. The first one is the melt and press method[Yamada & Kitayama, 1981]. The copolymer crystallizes into α or γ phases when it is slowly cooled to room temperature from the melt. The film has a high degree of crystallinity. Stretching or poling process is required to achieve the β phase crystals. For the melt and press fabrication process, the film thickness is usually > 1 μm. Spin coating from solution is another common fabrication method. By changing the weight percentage of the polymer in solution, spin coating can be used to produce films with thickness ≤100 nm. Different crystal phases can be achieved from polymer dissolved in different solvents. Spin coat from 2-butanone or cyclohexanone solutions allow the film to be crystallized into the β phase directly. Another method of making ultra thin film reported by A.V. Bune et al. [Bune et al., 1998] is Langmuir-Blodgett deposition, which results in films which are a few monolayers thick and can be switched at 1 V. After making the films, thermal annealing is always used to increase the degree of crystallinity. The annealing will be discussed in section 5.

### 3.2 Electrical characterization methods for polarization

The application of an electric field across the FeCap with an amplitude higher than the coercive field will reverse the polarity of the dipoles, and induce a switching current flow through the external closed loop. The total number of dipoles determines the electric displacements or polarization of the film. By integrating the switching current in the time domain, the total number of the switched dipoles or charges can be calculated. Two types of waveforms are commonly used to measure the polarization, the triangular wave for hysteresis loop characterization and a sequence of pulses for the standard Positive Up Negative Down (PUND) method [Kin et al, 2008; Mao et al., 2010b], as shown in figures 6 (a) and (b), respectively.

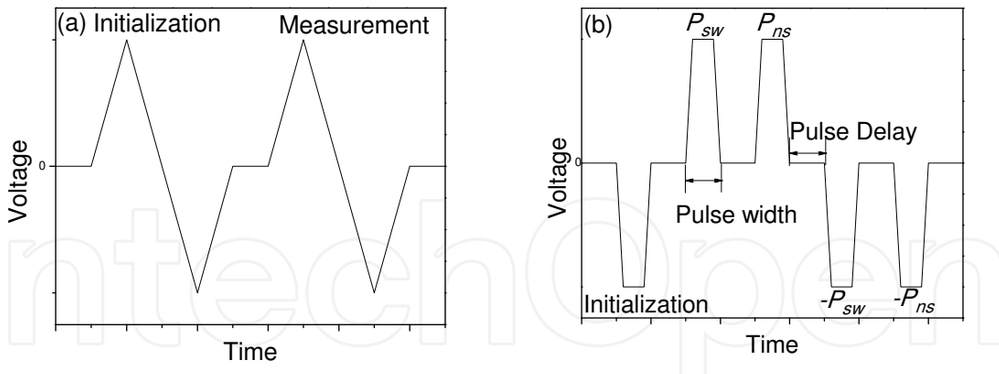


Fig. 6. The polarization measurement waveforms for (a) hysteresis loop and (b) PUND characterizations.

In the hysteresis loop measurement, the first triangular wave is used for initialization of the ferroelectric capacitor, followed by the second waveform for polarization measurement in both positive and negative directions. In the PUND measurement, switching polarization ($P_{sw}$) and nonswitching polarization ($P_{ns}$) are measured. $P_{sw}$ corresponds to the current integration in the polarization switching transient, and $P_{ns}$ corresponds to the current integration when the polarization has the same direction as the applied electric field. They are defined as [Mao et al., 2010b]

$$P_{sw} = P_s + P_r \quad (1)$$

$$P_{ns} = P_s - P_r \quad (2)$$

where $P_s$ and $P_r$ represent the spontaneous polarization and remanent polarization, respectively. The five sequential pulses represent initialization, measurement for $P_{sw}$, $P_{ns}$ in positive and negative directions, respectively.

### 3.3 Hysteresis loop measurement

The hysteresis loop is one of the most important tools to characterize ferroelectrics. A significant amount of information can be extracted from the hysteresis loop. Similar to other ferroelectrics, P(VDF-TrFE) copolymer exhibits remanent polarization. Figure 7 (a) shows the hysteresis loops measured at 1 Hz with different applied voltages for a FeCap with P(VDF-TrFE) film thickness of approximately 154 nm. As the voltage increases to 8 V, the FeCap starts to show hysteresis characteristics, and saturates at above 10 V. $P_s$ and +/-$P_r$ are plotted as a function of voltage in Figure 7 (b). $P_s$ and $P_r$ increase rapidly at voltage > 6 V, and saturate at 8.2 μC/cm² and 6.9 μC/cm², respectively. The coercive voltage ($V_c$) is defined as the voltage when $dP/dV$ reaches maximum, which is approximately 6.7 V, corresponding to a coercive field ($E_c$) of 0.44 MV/cm.

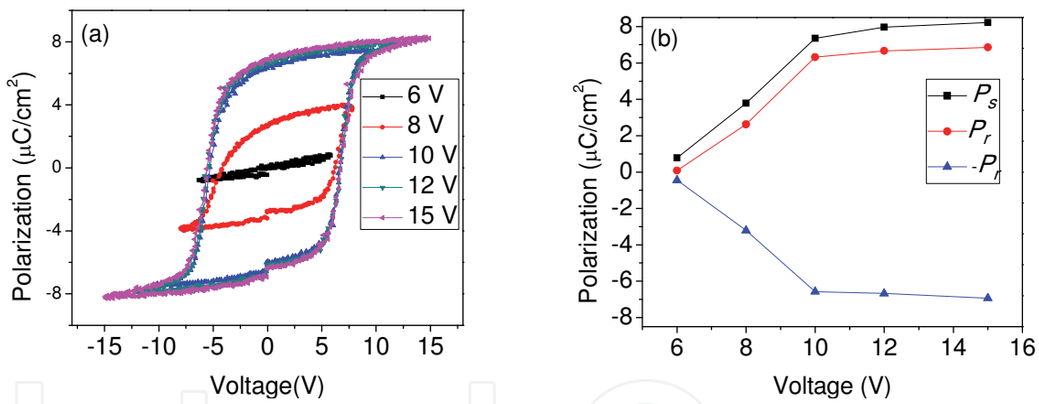


Fig. 7. (a) Hysteresis loops measured at different voltages for P(VDF-TrFE) FeCap, and (b) $P_s$ and +/-$P_r$ as a function of applied voltage.

### 3.4 PUND measurement

In the PUND method, a circuit is used to measure the currents in polarization switching and nonswitching transients, or measure the displacement and polarization of the FeCaps. In order to measure the polarization switching transient, we use a function generator to bias the FeCap, and measure the voltage across a linear resister using an oscilloscope, as shown in Figure 8. The transient current can be calculated by dividing the voltage with the resistance. $P_{sw}$ and $P_{ns}$ can be calculated by integrating the current in the time domain.

Typical PUND measurement data from a P(VDF-TrFE) based FeCap (size of 300μm × 300μm) are plotted in Figure 9. V1 and V2 represent the voltages measured from channel 1 and 2 of the oscilloscope, respectively. Rescaling V2 by 1/R (1000 ohms in the measurement) gives the transient current. The 1st, 3rd and 5th pulses induce large responses, representing

the polarization switching of the dipoles, while the 2nd, 4th, and 6th pulses correspond to the nonswitching transient with small current responses, because the dipoles have already aligned in the same direction as the applied electric field. The sharp response for polarization switching indicates the fast rotation of the dipoles, and the large difference between the switching and nonswitching responses indicates a large remanent polarization. $P_{sw}$ and $P_{ns}$ are calculated from the transient switching current to be 11.2 μC/cm² and 1.3 μC/cm², respectively. The switching current is a function of the applied electric field.

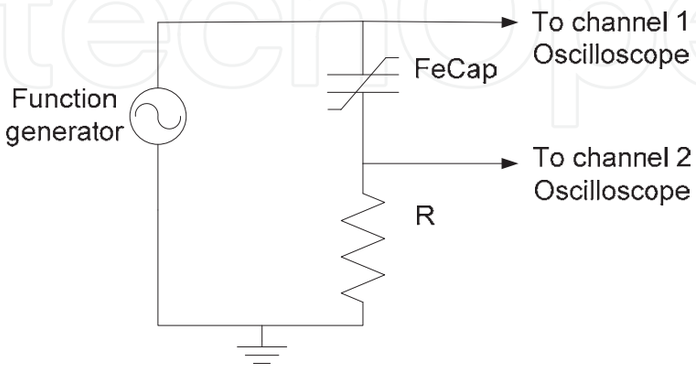


Fig. 8. The circuit schematic used to measure the currents in the switching and nonswitching transients using the PUND method.

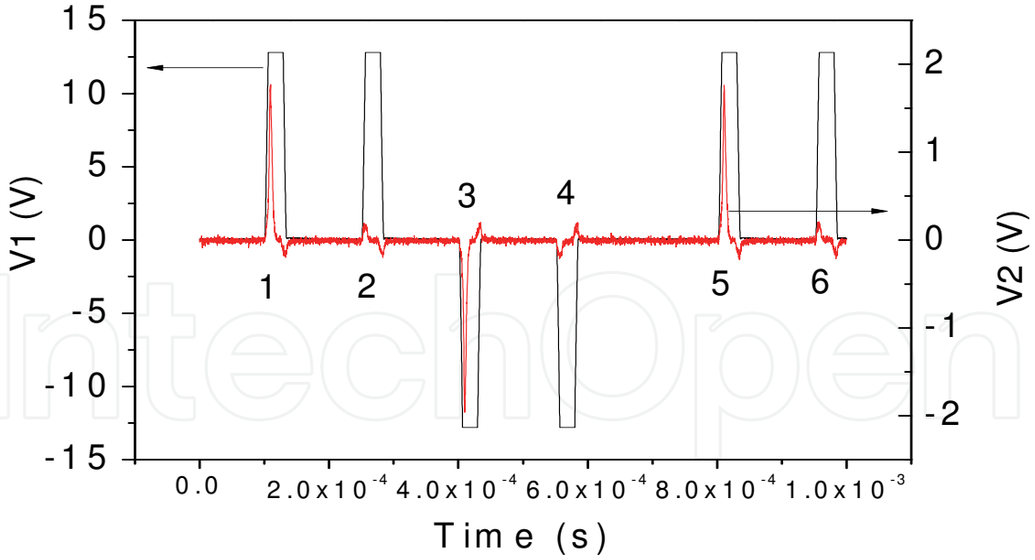


Fig. 9. The switching and nonswitching transient measurement of a P(VDF-TrFE) based FeCap using the PUND method.

### 3.5 Capacitance-voltage measurement

The nonlinearity of the dielectric response to electric field is also present in P(VDF-TrFE), as shown in Figure 10. An FeCap with P(VDF-TrFE) thickness of 154 nm is measured at 100

KHz. The dielectric permittivity is a function of $dP/dV$, which corresponds to the slope of the polarization-voltage plot. The dielectric constant is measured to be between 7.8 and 11, depending on the electric field [Mao et al., 2010a]. The peaks in the capacitance correspond to the polarization reversal of the dipoles, and the electric field for the peak capacitance corresponds to the coercive field [Lohse et al., 2001].

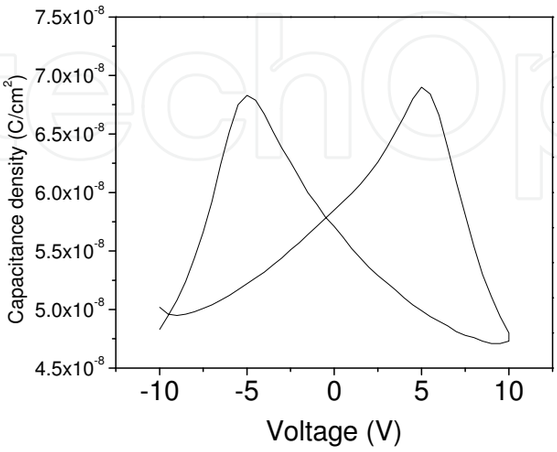


Fig. 10. The capacitance-voltage response of a 154 nm thick P(VDF-TrFE) based FeCap.

## 4. Polarization switching kinetics of P(VDF-TrFE) thin films

Understanding the kinetics of polarization switching is important to the application of ferroelectric materials. The polarization dipole reversal mechanism of inorganic ferroelectric materials such as lead zirconate titanate (PZT) has been studied for many years. The switching kinetics in a single crystal ferroelectric is found to follow the classical model called the Kolmogorov-Avrami-Ishibashi (KAI) model [Lohse et al., 2001; Tagantsev et al, 2002]. The KAI model was developed by the group of Ishibashi, based on the statistical theory of Kolmogorov and Avrami (KA) [Kolmogorov, 1937; Avrami 1939; Avrami 1940; Avrami 1941, as cited in Lohse et al., 2001], which was originally developed for the modeling of the crystallization process in metals. However, for polycrystalline ferroelectric thin films, the switching kinetics were frequently found to disobey the KAI model [Lohse et al., 2001; Tagantsev et al, 2002]. In this section, the polarization switching mechanism and the KAI model will be briefly discussed, and correlated with a model based on region-by-region switching for P(VDF-TrFE) thin films[Tagantsev et al, 2002]. Some alternative models for P(VDF-TrFE) will also be briefly introduced.

### 4.1 The polarization switching mechanism and KAI model

Ferroelectric polarization is defined as the electric dipole moment, or the displacement of charge density away from the center of the unit cell in the crystal lattice. The polarization direction can be switched by applying an electric field. The polarization switching process is commonly considered to be controlled by two mechanisms; domain nucleation and expansion [Merz, 1956; Kimura & Ohigashi, 1986]. The switching time is a function of the electric field, and for these two mechanisms, the switching time for each mechanism has a different dependence on the electric field. The domain nucleation process has an exponential relationship and can be expressed as [Merz, 1956]

$$\tau_0 = \tau_a e^{(E0/E)^n} \tag{3}$$

where $E_0$ is the activation field, $\tau_a$ is the switching time at $E = E_0$, which corresponds to the fastest switching speed of the material, and n is a constant related to the dimension of the domain growth. For domain expansion, the reciprocal of $1/\tau_0$ has a linear relationship as described in equation (4) [Merz, 1956];

$$\frac{1}{\tau_0} \sim \mu(E - E_1) \tag{4}$$

where μ is the mobility of the domain expansion and $E_1$ is a limiting electric field similar to a coercive field strength. The polarization switching of the ferroelectric is considered to be a combination of these two processes. Therefore, for a single crystal material, it exhibits a total switching time $\tau_0$, which is a function of applied electric field.

The KAI model describes the switching polarization phenomenon as initially being a uniform formation of the reversal nucleation centers, followed by the unrestricted expansion and overlapping of the domains throughout the sample. The volume of polarization can be mathematically expressed as [Lohse et al., 2001; Tagantsev et al, 2002];

$$p(t) = 1 - e^{-(t/\tau_0)^n} \tag{5}$$

where *p(t)* is the volume of the ferroelectric that has been switched in time *t*, $\tau_0$ is the switching time and n is a dimension constant. The electric displacement D can be expressed as [Tajitsu et al., 1987];

$$D = \varepsilon E + P = \varepsilon E + 2P_r(1 - e^{-(t/\tau_0)^n}) \tag{6}$$

where ε, E, P and $P_r$ are the linear dielectric permittivity, electric field, polarization and remanent polarization, respectively.

Due to the nature of polycrystalline ferroelectric thin films, the KAI assumptions are not always met. It was observed in many cases that the switching time increases and the distribution of the switching time broadens as the film thickness decreases [Lohse et al., 2001; Tagantsev et al, 2002]. In the P(VDF-TrFE) system, Tajitsu et al. proposed that the increase of switching time for thinner films correspond to the increase in the activation field, which is caused by the formation of a surface layer [Tajitsu, 1995]. Nakajima et al, found that the increase in the switching time happens for FeCaps with Al contacts, but for Au contact FeCaps, the switching time is independent with film thickness [Nakajima et al., 2005]. The film thickness and contact dependence of polarization switching will be discussed in section 5. To explain the broadening of the switching time distribution for P(VDF-TrFE) thin films, alternate methods have been proposed to model the polarization switching kinetics. They are introduced and discussed below.

### 4.2 Region-by-region switching

The polarization switching process in a ferroelectric is affected by many factors, especially the nucleation rate of reversal domains, domain dimension, and the mobility of the domain wall [Tagantsev et al, 2002]. Different from single crystal materials, AFM and TEM studies

suggest that the switching process in thin films occur region-by-region [Colla et al., 1998; Ganpule et al. 2000; Kim et al., 2010]. The polarization switching process in one region does not necessarily expand through the neighboring regions and switch the whole film. Therefore, the switching of each region is independently determined by its own characteristics, such as nucleation rate and domain dimension. Based on this analysis, Tagantsev et al proposed a model called nucleation-limited-switching (NLS) for the polarization switching of a ferroelectric thin film [Tagantsev et al, 2002]. In this model, the assumption is that each region switches independently, and in each region, the switching process is dominated by the nucleation time of the first reversal domain. The switching of the whole system is controlled by the statistics of domain nucleation, instead of domain expansion in the KAI model.

For the P(VDF-TrFE) copolymer, polarization reversal originates from the rotation of the carbon-fluorine and carbon-hydrogen covalent bonding around the central chain of the polymer [Furukawa et al., 2006]. In thin film P(VDF-TrFE), the activation field for domain expansion is small (approximately 0.87 MV/cm) [Kim et al., 2010] compared to domain nucleation (approximately 7.8-12 MV/cm) [Tajitsu, 1995; Nakajima et al., 2005; Kusuma et al., 2010]. Therefore, the polarization switching dynamics are dominated by domain nucleation. Because of polycrystalline nature of thin films, they consist of many grains separated by grain boundaries. The NLS model better describes the switching process of this system. Therefore, it can be used to model the switching polarization as a function of time [Mao et al., 2010b].

In Figure 11, $P_s$ is shown as a function of time for a FeCap with a P(VDF-TrFE) film thickness of 100 nm using the PUND method. The experimental data and the calculated response using the NLS model are plotted as symbols and solid lines, respectively. The polarization dispersion at a pulse width equal to 1 s (corresponding to log (t) = 0) is due to the high dc conductance of the devices caused by the increased dielectric leakage at high voltage and low frequencies [Nakajima et al., 2005]. These points are not included in the model calculation. The agreement between the experimental data and the model suggests the region-by-region polarization switching process in P(VDF-TrFE) system is a reasonable description.

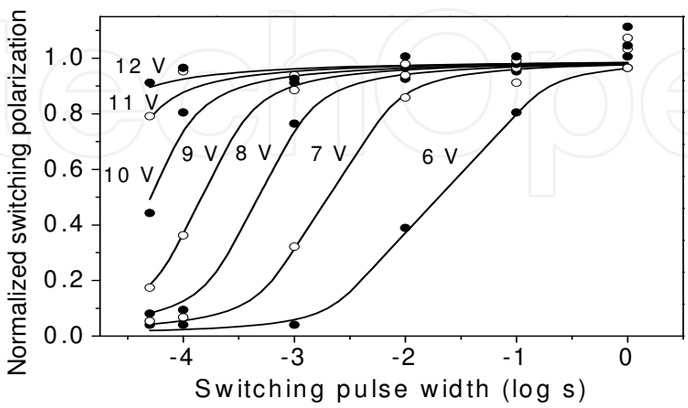


Fig. 11. The relationship of the normalized switching polarization and applied voltage pulse width in positive region. The symbols are experimental data and the lines are the calculated response using the NLS model. Reprinted from [Mao et al, 2010b] with permission.

Since the nucleation limited switching dynamic of P(VDF-TrFE) thin film dominate this switching polarization, the polarization switching time (τ) can be described as the delay time for domain nucleation, while the time for domain expansion can be neglected. The difference in domain dimensions, region sizes and especially the distribution of the nucleation centers and the nucleation rate of the reversal polarization among each region leads to a distribution of switching times throughout the film. For each region, τ is a function of applied voltage, characterized by an individual activation voltage ($V_0$). The dispersion of τ, characterized by $\tau_{max}$ and $\tau_{min}$, corresponding to the maximum and minimum $V_0$ among all regions in the film can be extracted from the model and plotted as a function of applied voltage (symbols), as shown in Figure 12. The exponential relationship of τ and applied voltage follows equation (3). $\tau_{max}$ is used to fit equation (3) (plotted as the solid line in Figure 12), $\tau_0$ and $E_0$ can be extracted as 5 ns and 9.6 MV/cm.

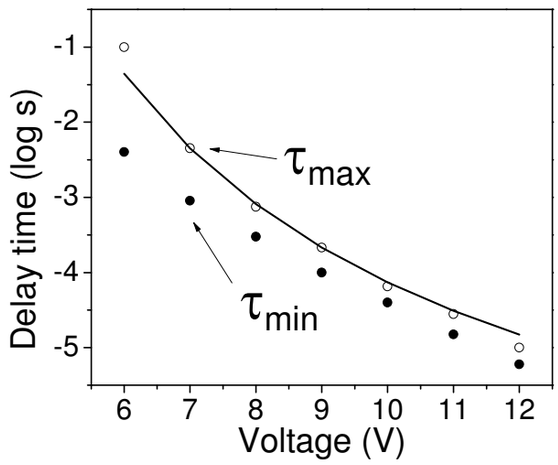


Fig. 12. Experimental $\tau_{max}$ and $\tau_{min}$ data from Figure 11 plotted as a function of applied voltage, and the fitting for $\tau_{max}$ in positive polarization region. Reprinted from [Mao et al, 2010b] with permission.

Figure 11 shows the switching dynamics (+/-$P_{sw}$ versus time) for P(VDF-TrFE) with a distribution as long as three decades, compared to eight decades for the 135 nm $Pb(Zr,Ti)O_3$ system reported in the literature[Tagantsev et al, 2002]. The reduced range of switching dynamics in P(VDF-TrFE) films indicates a more uniform distribution of switching time, or activation field among the regions. One of the reasons could be the more uniform size of the regions and distribution of nucleation centers within the regions. Additionally, P(VDF-TrFE) has a much higher activation field of 9.6 MV/cm compared to $Pb(Zr,Ti)O_3$, 0.77 MV/cm, therefore, the reversal polarization domain nucleation kinetics at room temperature for P(VDF-TrFE) are less dependent on thermal activation [Stolichnov et al., 2003; Mao et al., 2010b]

### 4.3 Surface roughness based model

As the film thickness decreases, the surface roughness becomes significant, resulting in a non-uniform electric field distribution. For the broadening of the switching time distribution, Nakajima et al proposed a model based on surface roughness [Nakajima et al., 2005]. The non-

uniform distribution of electric field on the ferroelectric thin film leads to different values of switching time on different regions, and causes the broadening of the switching time.
Using this method, the authors plotted the thickness distribution vs. average film thickness of four P(VDF-TrFE) samples (symbol) and fit the data with the Gaussian distribution function (line); as shown in Figure 13 (a). The electric field distribution across the film surface can be determined, which is correlated to the switching time using equation (3). The electric displacement D and polarization P can be calculated using equation (6). The calculated switching time distributions for different film thicknesses are plotted in Figure 13 (b) [Nakajima et al., 2005]. As seen for the 50 nm P(VDF-TrFE) films, the maximum amplitude of the surface roughness is approximately 20 nm, which causes a significant broadening of the switching time distribution, based on the model calculation shown in Figure 13 (b). Compared to the experimental results in Figure 19 (a) by the authors, the model predicts the correct trend, but the predicted distribution is slightly broader.

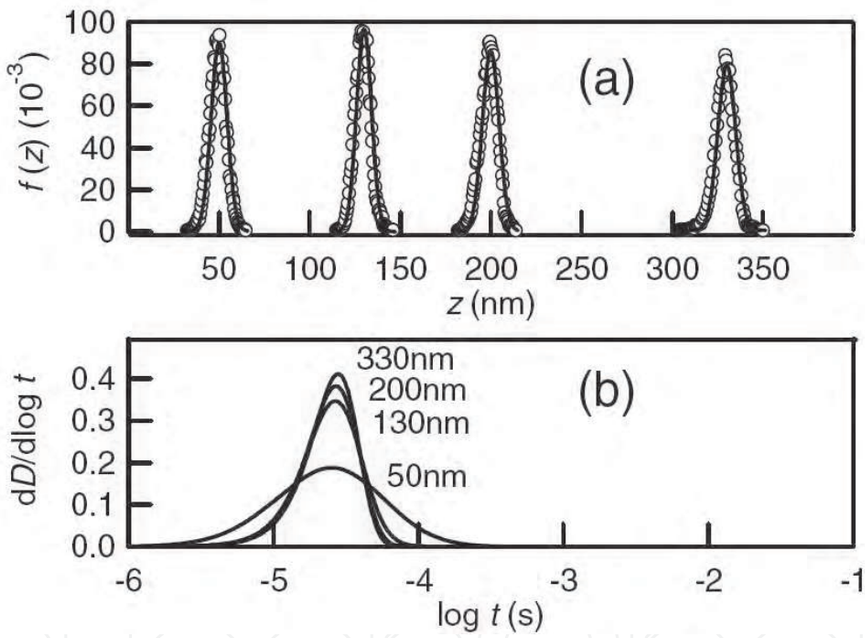


Fig. 13. The surface roughness for (a) The thickness distribution vs. the average film thickness of four P(VDF-TrFE) (75/25) copolymer thin films from 50-330 nm, and (b) the calculated differential switching time distribution at electric field of 120 MV/m. Reprinted from [Nakajima et al., 2005] with permission.

### 4.4 Other model for P(VDF-TrFE) thin films

The switching kinetics of P(VDF-TrFE) thin films were also studied by Kimura et al [Kimura & Ohigashi, 1986], who proposed a model based on the defects in the crystalline phase. The defects can modulate the local electric field in the surrounding material and prevent domain growth. The effect of defects can be described as a dipole moment $\Delta\mu$, therefore, the C-F dipole moment can be affected by the defects and deviated from its intrinsic value. The $\Delta\mu$ is non-uniformly distributed, which can broaden the distribution of switching time in the film [Kimura & Ohigashi, 1986].

## 5. Annealing, film thickness and contact dependence

The fabrication process and device structure are significant factors that need to be understood to optimize device performance. Thermal annealing, P(VDF-TrFE) film thickness and contacts are discussed in this section.

### 5.1 Thermal annealing

The main purpose for annealing P(VDF-TrFE) films is to increase the degree of crystallinity of the β phase and remove the residual solvent in the film [Mao et al., 2010a]. The microstructure and electrical performance of the polymer are related to the annealing temperature, time and temperature ramp up and cool down rate. The two phase transition temperatures, the Curie temperature ($T_c$) and the melting temperature ($T_m$) are critical in the annealing process [Mao et al., 2010a]. When heating above $T_c$, the ferroelectric materials loses spontaneous polarization and becomes paraelectrics. It is necessary to anneal the sample in the paraelectric phase, since the thermal energy allows the polymer chains to rearrange their orientation and position to form a more crystalline structure after cooling [Furukawa et al, 2006]. For P(VDF-TrFE) copolymer, if the films are annealed at temperatures above $T_m$, the β phase decreases and recrystallizes into the α or γ phase when slowly cooled down. Therefore, to achieve high β phase crystallinity films of P(VDF-TrFE), $T_c < T_{anneal} < T_m$ is required for annealing.

The annealing effects on the microstructure of the P(VDF-TrFE) film can be studied from the point of view of surface morphology, degree of crystallinity and molecular chain orientation. The characteristics of the β phase P(VDF-TrFE) have been discussed in section 2. For 70/30 P(VDF-TrFE) films ($T_c$=118 °C, $T_m$ =144 °C) annealed at temperatures below $T_m$, increasing the annealing temperature causes a dramatic increase in grain size, as shown in the AFM height images in Figure 14 (a)-(d). The increase in the crystallinity of β phase is reflected in the XRD results, as the diffraction intensity increased for the (110), (200) diffraction peaks at 2θ=19.9°, which is shown in Figure 15. When annealed above $T_m$, the β phase grains disappeared and the characteristics of the surface morphology change significantly (Figure 14 (e)). The melting and recrystallization process are also recognized as a decrease of the crystallinity of β phase in XRD data (Figure 15). The surface roughness increases dramatically as the annealing temperature increase above $T_c$ [Mao et al., 2010a].

The effects of annealing on molecular bond and polymer chain orientation can be clearly detected using polarized FT-IR, as discussed in section 2. Figure 16 [Mao et al. 2010a] shows the p-polarized FT-IR results for the P(VDF-TrFE) film annealed at different temperatures. When annealed below $T_c$ (at 65 °C), the molecular and polymer chains do not have sufficient energy to align, therefore, they have a random orientation, as shown by the low IR absorption at 850 and 1288 $cm^{-1}$. When annealed above $T_c$ but below $T_m$, the higher thermal energy allows the polymer chains to start to reorient and align parallel to the substrate, as indicated by the increase of the IR absorption at 850 and 1288 $cm^{-1}$ (118-144 °C). Annealing above $T_m$, the polymer chains start to rotate and partially align normal to the substrate, and the β phase decreases, observed by the increase of the IR absorption at 1400 $cm^{-1}$ and the decrease of the 850 and 1288 $cm^{-1}$ bands.

For the electrical properties of P(VDF-TrFE) FeCaps, $P_s$, $P_r$ and $E_c$ of the FeCap depend mainly on the molecular and polymer chain orientation of the β phase crystals, as shown in Figure 17. The FeCaps were annealed at different temperature before the deposition of the top contacts. In Figure 17, FeCaps annealed below $T_c$ or above $T_m$ show low $P_s$, $P_r$ and large

$E_c$. When annealed between $T_c$ and $T_m$, high $P_s$, $P_r$ and low $E_c$ are achieved, with negligible difference as a function of temperature.

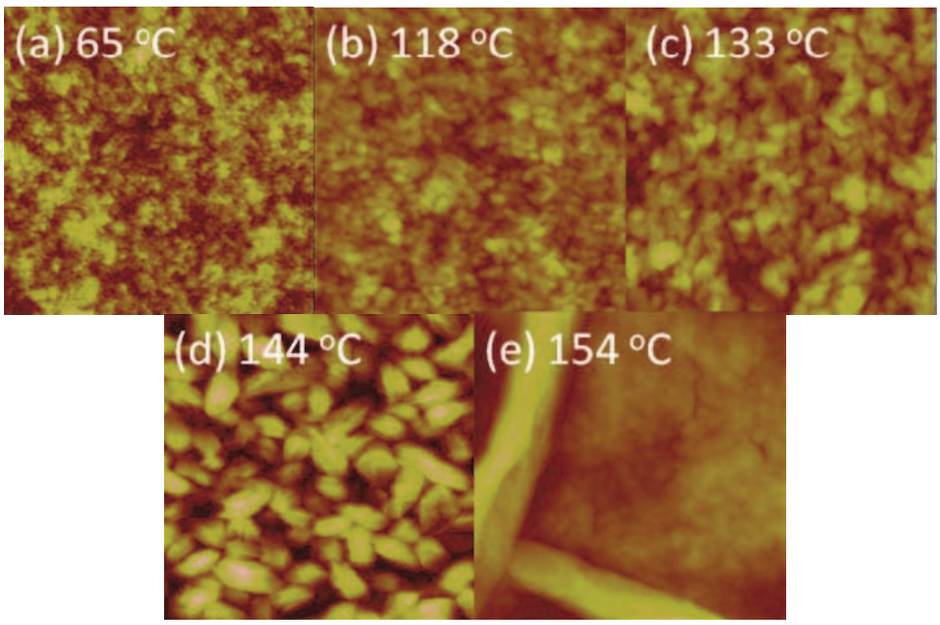


Fig. 14. AFM 1μm×1μm height images of P(VDF-TrFE) film annealed at different temperatures. (a) 65 °C, (b) 118 °C, (c) 133 °C, (d) 144 °C, and (e) 154 °C. The height scales are 30 nm for (b), (c), (d), 10 nm for (a), and 100 nm for (e). All of the images were collected at room temperature.

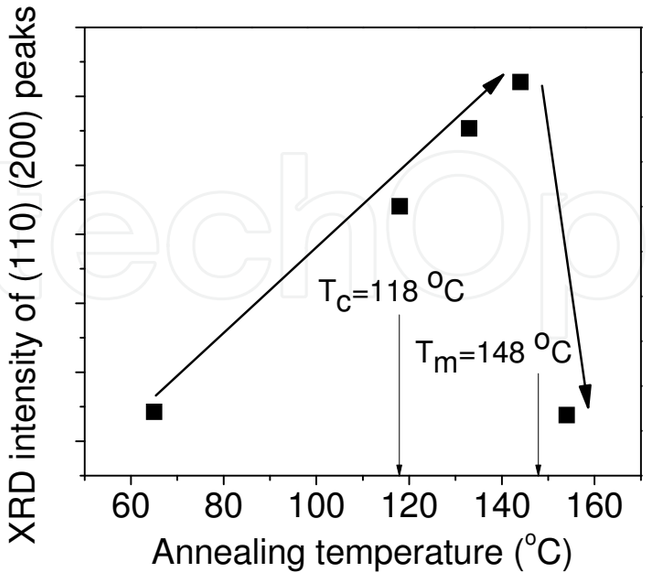


Fig. 15. XRD intensity of (110), (200) orientations after different annealing temperatures. The (110), (200) diffraction peaks at 2θ=19.9° are attributed to the β phase of P(VDF-TrFE).

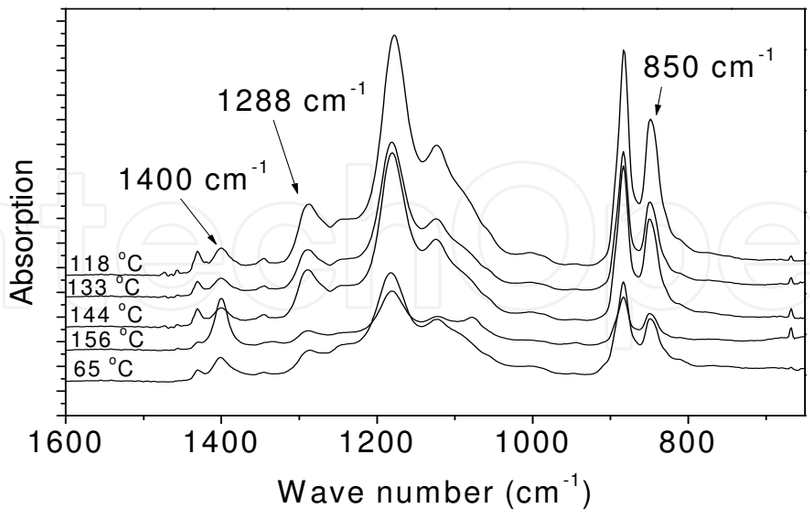


Fig. 16. Polarized FT-IR results for P(VDF-TrFE) films annealed at different temperatures. The different absorption at 850, 1288 and 1400 $cm^{-1}$ bands represent the annealing temperature affects on polymer chain alignment. Reprinted from [Mao et al., 2010a] with permission.

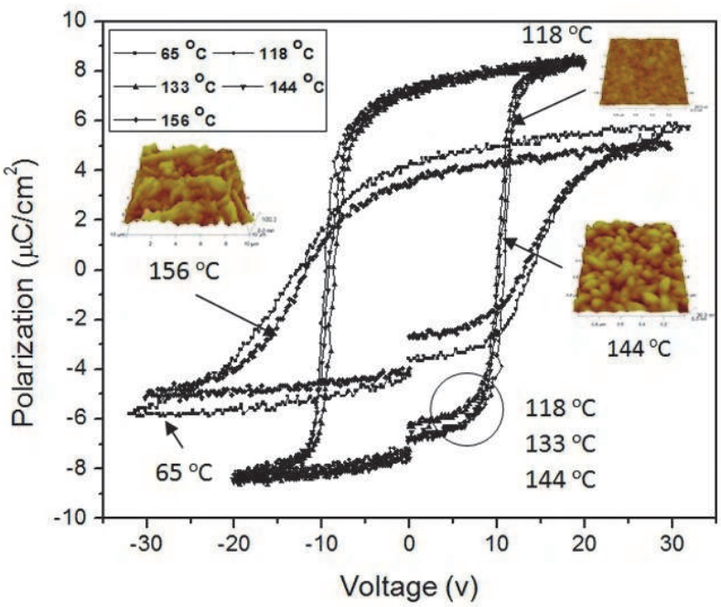


Fig. 17. The hysteresis loops of P(VDF-TrFE) FeCaps annealed at different temperatures. Reprinted from [Mao et al., 2010a] with permission.

### 5.2 P(VDF-TrFE) film thickness dependence

For P(VDF-TrFE) copolymers, $E_c$ is large, approximately 0.5 MV/cm, and depends on the VDF/TrFE ratio. For low voltage applications, it is necessary to reduce the film thickness,

while maintaining good ferroelectric properties. It has been shown that as the film thickness decreases, the grain size decreases, along with a decrease in the degree of crystallinity [Mao et al., 2010a]. The x-ray diffraction angle (2θ) for the (110) (200) orientation of the β phase remains constant, indicating that the inter-planar spacing, b, in the crystal lattice does not change for thinner films [Mao et al., 2010a].

Merz studied the film thickness dependence of switching kinetics for $BaTiO_3$ crystals and found the activation field increases as the film thickness decreases, which is attributed to the formation of an interfacial layer between the ferroelectric crystal and the contacts [Merz, 1956]. Based on Merz's approach, Tajitsu [Tajitsu, 1995] and Xia et al [Xia et al., 2001] studied the switching kinetics of P(VDF-TrFE) FeCaps with Al contacts for different ferroelectric film thicknesses. Their experimental data suggest that the increase in polarization switching time as the P(VDF-TrFE) film thickness decreases can possibly be explained by the formation of an interfacial layer.

In Merz's approach, the thickness dependence of $E_0$ for thin films can be expressed as [Merz, 1956]

$$E_0 = E_{01} + \left(\frac{\beta}{d}\right) \tag{7}$$

where $E_{01}$ is the activation field for thick films, β is an experimental fitting parameter and d is the film thickness.

The interfacial layer can be treated as a dielectric layer electrically connected in series with the ferroelectric film; therefore, from [Merz, 1956]

$$V_{total} = V_f + V_{it} \tag{8}$$

where $V_{total}$, $V_f$ and $V_{it}$ are the total applied voltage, voltage drop across the ferroelectric film and the interfacial dielectric layer, respectively. The charge continuity at the boundary of the two interfaces can be expressed as [Merz, 1956]

$$\frac{V_{total}}{V_f} = \frac{\varepsilon_f \cdot d_{it}}{\varepsilon_{it} \cdot d_f} + 1 \tag{9}$$

where $\varepsilon_f$ and $\varepsilon_{it}$ are the dielectric permittivity of the ferroelectric and interfacial layers, $d_f$ and $d_{it}$ are the thickness of the ferroelectric and interfacial layers, respectively. Due to $d_f >> d_{it}$ and $\varepsilon_f/d_f << \varepsilon_{it}/d_{it}$ [Xia et al., 2001], (9) can be rewritten as [Xia et al., 2001]

$$E_f = E_{total}\left(1 - \frac{\varepsilon_f \cdot d_{it}}{\varepsilon_{it} \cdot (d_f + d_{it})}\right) \tag{10}$$

where $E_f$ and $E_{total}$ are the electric field across the ferroelectric material and the applied electric field.

Xia et al characterized P(VDF-TrFE) FeCaps with the film thickness ranged from 600 to 120 nm, and used this approach to analyze the switching time dependence. If the interfacial model is not incorporated, a clear thickness dependence of switching time can be found (Figure 18 (a)), as the switching time increases for thinner films. When the interfacial layers are taken into account, switching time is much less dependent on film thickness, as shown in Figure 18 (b).

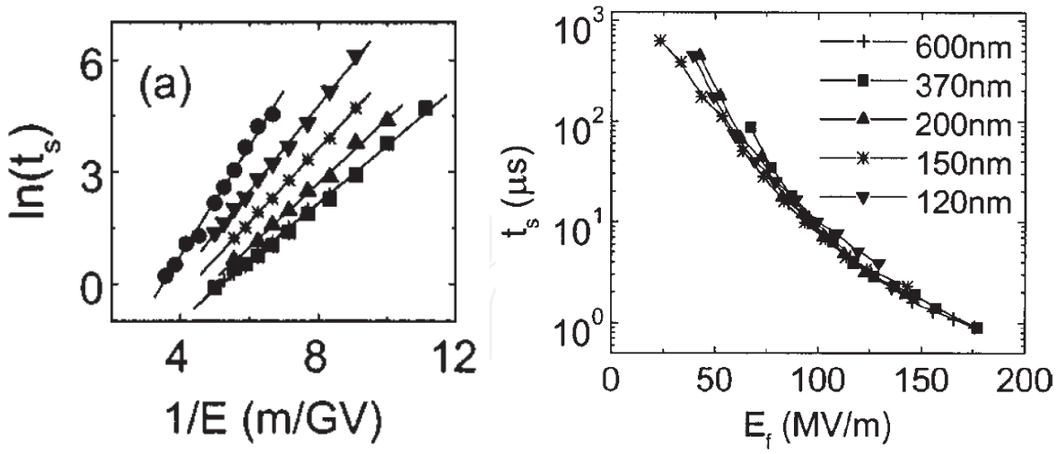


(a) (b)

Fig. 18. (a) Switching time as a function of 1/E with different film thicknesses for (from right to left) 600, 370, 200, 150, 120 nm films and (b) switching time as a function of $E_f$ using the interfacial layer model. Reprinted from [Xia et al., 2001] with permission.

### 5.3 Contact dependence

Metal is the most commonly used material for FeCap contacts. For organic electronic systems, the physical and chemical processes on the interface need to be considered when metal is deposited on the organic materials. Reactive metals such as Ti, Ni and Al can react with the organic materials and form an interfacial layer, which can degrade the electrical properties [Xu et al., 2009]. For P(VDF-TrFE) copolymer, Ti and Ni can react with the fluorine atom in the $-CF_2-$ components and create $TiF_x$ and $NiF_x$ at the interface, respectively [Xu et al., 2009; Chen & Mukhopadhyay, M., 1995]. For chemically inert metals, such as Au, less chemical reaction occurs between the metal atom and P(VDF-TrFE). However, it is easy for the metal to diffuse into the low density polymer film, creating a large leakage current for thinner films.

Nakajima et al studied the P(VDF-TrFE) FeCaps using different contact metals as Al and Au. The switching time distribution broadens as the film thickness decreases for FeCap with both contacts. However, the authors found that the switching time increase with decreasing film thickness only for the FeCaps with Al contact, not for Au contact FeCaps. The authors suggest that the increase of the switching time is attributed to an interfacial dielectric layer formed when Al is deposited on P(VDF-TrFE), which is in agreement with the above discussion. This interfacial layer helps reduce the leakage current, while degrading the polarization switching speed. No interfacial layer is formed between P(VDF-TrFE) and Au. Therefore, the switching time does not increase with decreasing film thickness.

It has also been demonstrated that by using polymeric electrodes, device performance and reliability can be improved. The improvement can be attributed to better adhesion, wetting and similar chemical properties of the surface, compared to metal contacts. Naber et al found that adding a conducting polymer poly(3,4-ethylenedioxythiophene): poly(styrenesulfonicacid) (PEDOT: PSS) on top of Al or indium-tin-oxide (ITO) for bottom contact improves both the $P_r$ and switching time for films as thin as 65 nm of P(VDF-TrFE) [Naber et al., 2004]. Xu et al demonstrated that both polypyrrole-poly(styrene sulfonate) and

PEDOT-PSSH can be used as buffer conducting polymer layers for P(VDF-TrFE) top and bottom contacts. Improved device performance with higher $P_r$ and faster switching speeds were achieved. A $P_r$ of more than 70% of its initial value can be achieved after $1\times10^7$ cycles of switching for 50 nm thick P(VDF-TrFE) film devices, as shown in Figure 20 [Xu et al., 2007, 2009]. Xu et al also found that the conducting polymer buffer layers improve the degree of crystallinity of the thin films [Xu et al., 2009].

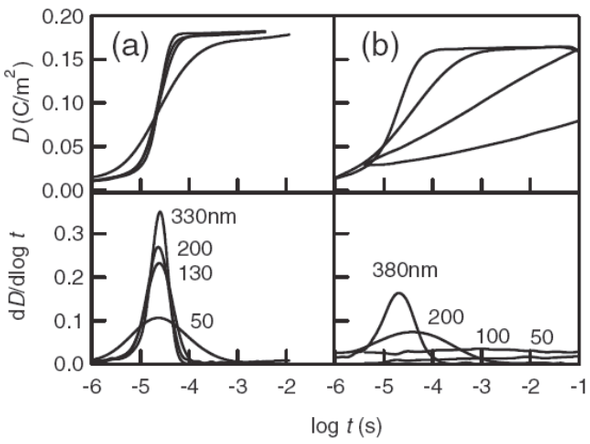


Fig. 19. The polarization switching behaviors for (a) Au contact FeCap, and (b) Al contact FeCaps. Reprinted from [Nakajima et al., 2005] with permission.

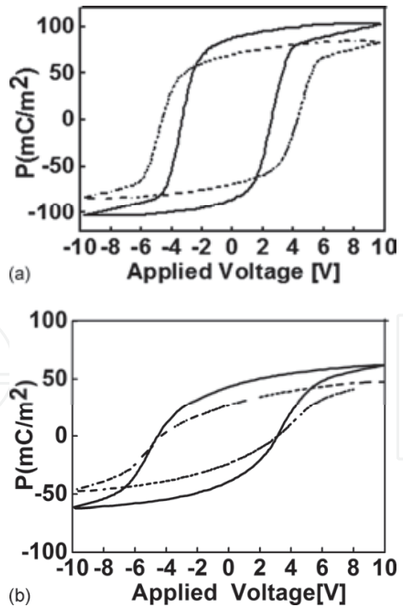


Fig. 20. Hysteresis loops for 50 nm of P(VDF-TrFE) film with Ti as the top and bottom contacts; (a) with two PEDOT-PSSH buffer layers between P(VDF-TrFE) and Ti for top and bottom contacts, (b) without buffer layers. Solid lines and dashed lines are the measurement before and after $1\times10^7$ cycles of switching, respectively. Reprinted from [Xu et al., 2009] with permission.

## 6. Conclusions

In this chapter, the material and electrical properties, and the ferroelectric polarization switching kinetics of P(VDF-TrFE) copolymer have been reviewed. The ferroelectric properties originate from the large difference in the electronegativity between the fluorine, carbon and hydrogen atoms. The polymer phase structure, surface morphology, crystallinity, and molecular chain orientation associated with the ferroelectric β phase have been discussed. The P(VDF-TrFE) copolymer exhibits a high spontaneous polarization > 8 μC/cm² (depending on fabrication process and mole ratio of VDF/TrFE) and a square like hysteresis loop. The sharp peak in the switching current indicates the fast rotation of the dipole around the polymer chain.

To illustrate the switching kinetics of P(VDF-TrFE) thin films, two basic polarization switching mechanisms, reversal polarization nucleation and domain wall expansion were reviewed. A commonly accepted statistical model (KAI) for single crystal polarization switching was discussed and extended to models to explain the switching time broadening for P(VDF-TrFE) thin films, including the nucleation-limited-switching (NLS) model based on region-to-region switching kinetics, surface roughness based model, etc. The NLS model can be successfully used to fit P(VDF-TrFE) switching data and $\tau_0$ and $E_0$ can be extracted as 5 ns and 9.6 MV/cm.

The annealing temperature, film thickness and contacts were then discussed. For annealing above $T_c$ but below $T_m$, the grain size and the crystallinity of the (110) (200) orientation of the β phase increases, the polymer chains align parallel to the substrate with the polarization dipole moment perpendicular to the substrate. At annealing above $T_m$, the surface morphology changes significantly, the degree of crystallinity in the β phase decreases dramatically, and the polymer chains tend to align normal to the substrate. As the film thickness decreases, the grain size and degree of crystallinity decrease. The increase switching time as film thickness decreases can possibly be explained by the formation of an interfacial layer. For the contact, reactive metals induce an interfacial layer, which causes an increase in the switching time. P(VDF-TrFE) FeCaps with Au contacts do not have this film thickness effect, but as the film becomes thinner than 100 nm, the diffusion of Au atoms increases the leakage current. Therefore, thin films with high quality are required. Using conducting polymers, such as PEDOT: PSS and polypyrrole-poly(styrene sulfonate) as a buffer layer for the contacts show improved electrical performance in remanent polarization, switching time and reliability for thin film P(VDF-TrFE) based FeCaps.

One of the most important applications of P(VDF-TrFE) copolymer is ferroelectric nonvolatile memory (FeRAM). The two stable states of the ferroelectric material in positive and negative directions can be used as digital data “1” and “0”, and the remanent polarization leads to data storage with the power off (nonvolatile). Due to the low temperature, solution process of P(VDF-TrFE) films, it is compatible with large area and flexible electronic applications. Even though the polarization switching speed of P(VDF-TrFE) is slow (~1 μs) compared to PZT (~ 10 ns), it is much faster than the conventional flash memory(100 μs) in writing and programming. Moreover, it is reliable with more than $1\times10^7$ cycles of switch [Mao et al., 2011a], and can be used in low voltage applications [Fujisaki et al., 2007]. The memory cell can be constructed by combining access transistors with the ferroelectric capacitors. The circuit structure depends on the number of access transistors and ferroelectric capacitors [Arimoto & Ishiwara, 2004]. One transistor-one capacitor (1T1C) FeRAM elements based on P(VDF-TrFE) were recently demonstrated by the authors [Mao,

et al., 2011b]. Ferroelectric transistors can also be fabricated using P(VDF-TrFE) for each bit in FeRAM [Naber et al., 2005; Lee et al., 2009], however, the reliability still needs to be improved for future applications.

## 7. Acknowledgements

The work at UT Dallas was partially financial supported by the Army Research Laboratory (ARL). The authors would also like to thank Dr. Scott R. Summerfelt of Texas Instruments and Dr. Eric Forsythe from ARL for many helpful discussions.

## 8. References

Arimoto, Y. & Ishiwara, H., (2004). Current status of ferroelectric random-access memory, *MRS Bulletin*, Vol. 29, No. 11, pp. 823-828, doi: 10.1557/mrs2004.235Bergman,

J. G.; Jr. McFee, J. H. & Crane, G. R., (March 1971) Pyroelectricity and Optical Second Harmonic Generation in Polyvinylidene Fluoride Films, *Appl. Phys. Lett.*, Vol 18, No. 5, pp. 203-205

Bune, A. V.; Fridkin, V. M.; Ducharme, S.; Blinov, L. M.; Palto, S. P.; Sorokin, A. V.; Yudin, S. G. & Zlatkin, A., (1998) Two-dimensional ferroelectric films, *Nature*, Vol. 391, No. 6670, pp. 874-877

Chen, T. C. S. & Mukhopadhyay, S. M., Metallization of electronic polymers: A comparative study of Polyvinylidene fluoride, polytetrafluoroethylene, and polyethylene, *J. Appl. Phys*., Vol. 78, No. 9, pp. 5422-5426

Colla, E. L.; Hong, S.; Tagantsev, A. K.; Setter, N. & No, K., (1998). Direct observation of region by region suppression of the switchable polarization (fatigue) in Pb(Zr, Ti)$O_3$ thin film capacitors with Pt electrodes, *Appl. Phys. Lett.,* Vol. 72, No. 21, pp. 2763-2765

Fujisaki, S.; Ishiwara, H. & Fujisaki, Y. (2007). Low-voltage operation of ferroelectric poly(vinylidene fluoride-trifluoroethylene) copolymer capacitors and metal-ferroelectric-insulator-semiconductor diodes, *Appl. Phys. Lett.,* Vol. 90, p. 162902

Furukawa, T.; Nakajima, T. & Takahashi, Y., (2006). Factors governing ferroelectric switching characteristics of thin VDF/TrFE copolymer films, *IEEE Trans. Dielectr. Electric. Insul.,* Vol. 13 No. 5, pp. 1120-1131, ISSN: 1070-9878

Ganpule, C. S.; Nagarajan, V.; Li, H.; Ogale, A. S.; Steinhauer, D. E.; Aggarwal, S.; Williams, E.; Ramesh, R & Wolf P. De, (2000). Role of 90 domains in lead zirconate titanate thin films, *Appl. Phys. Lett.,* Vol. 77, No. 2, pp. 292-294

Glass, A. M., (December 1971). Pyroelectric Properties of Polyvinylidene Fluoride and Its Use for Infrared Detection, *J. Appl. Phys*., Vol. 42, No. 13, pp. 5219-5222

Hu, Z. J.; Tian, M. W; Nysten, B. & Jonas, A. M., (2009). Regular arrays of highly ordered ferroelectric polymer nanostructures for non-volatile low-voltage memories, *Nat. Mater.* Vol. 8, No. 1, pp. 62-67

Kawai, H. (1969). The Piezoelectricity of Poly(vinylidene Fluoride), *Jpn. J. Appl. Phys.,* Vol. 8, pp. 975-976

Kepler, R. G, Ferroelectric, pyroelectric, and piezoelectric properties of poly(vinylidene fluoride), In: *Ferroelectric polymers chemistry, physics, and applications,* Hari Singh Nalwa, pp. 183-232, Marcel Dekker, Inc., New York

Kimura, K. & Ohigashi, H., (1986). Polarization behavior in vinyledene fluoride-trifluoroethylene copolymer thin films, *Jpn. J. Appl. Phys.,* Vol. 25, No. 3, pp. 383-387

Kim, K. J.; Reynolds, N. M. & Hsu, S. L. (1989). Spectroscopic analysis of the crystalline and amorphous phases in a vinylidene fluoride/trifluoroethylene copolymer, *Macromolecules,* Vol. 22, No. 12, pp. 4395-4401

Kim, Y.; Kim, W.; Choi, H.; Hong, S.; Ko, H.; Lee, H. & No, K., (2010). Nanascale domain growth dynamics of ferroelectric poly(vinylidene fluoride-co-trifluoroethylene) thin films, *Appl. Phys. Lett.*, Vol. 96, No. 1, p. 012908

Kin, N.; Takai, K. & Honda, K., (2008). High speed pulse measurement of micro ferroelectric capacitors using a multi-probe atomic force microscope, *Jpn. J. Appl. Phys.,* Vol. 47, No. 6, pp. 4638-4642

Kobayashi, M.; Tashiro, K. & Tadokoro, H., (1975). Molecular vibrations of three crystal forms of poly(vinylidene fluoride), *Macromolecules,* Vol. 8, No. 2, pp. 158-171

Kusuma, D. Y.; Nguyen, C. A. & Lee, P. S., (2010). Enhanced ferroelectric switching characteristics of P(VDF-TrFE) for organic memory devices, *J. Phys. Chem B,* Vol. 114, No. 42, pp. 13289-13293

Lee, K. H.; Lee, G.; Lee, K.; Oh, M. S. & Im, S., (2009). Flexible low voltage nonvolatile memory transistors with pentacene channel and ferroelectric polymer, *Appl. Phys. Lett.,* Vol. 94, No. 9, p. 093304

Lohse, O.; Grossmann, M.; Boettger, U.; Bolten. D. & Waser, R., (2001). Relaxation mechanism of ferroelectric switching in Pb(Zr,Ti)$O_3$ thin films, *J. Appl. Phys.,*Vol. 89, No. 4, pp. 2332-2336

Mao, D; Quevedo-Lopez, M. A.; Stiegler, H.; Alshareef, H. N. & Gnade, B. E., (2010). Optimization of poly(vinylidene fluoride-trifluoroethylene) film as non- volatile memory for flexible electronics, *Org. Electron*. Vol. 11, No. 5, pp. 925-932

Mao, D.; Mejia, I.; Stiegler, H.; Gnade, B. E. & Quevedo-Lopez, M. A., (2010) Polarization behavior of poly(vinylidene fluoride-trifluoroethylene copolymer ferroelectric thin film capacitors for nonvolatile memory application in flexible electronics, *Org. Electron.,* Vol. 108, No. 9, p. 094102, doi:10.1063/1.3500428

Mao, D.; Mejia, I.; Stiegler, H.; Gnade, B. E.; Quevedo-Lopez, M. A., (2011). Fatigue characteristics of Poly(vinylidene fluoride-trifluoroethylene) copolymer ferroelectric thin film capacitors for flexible electronics memory applications, submitted to *Org. Electron*.

Mao, D.; Mejia, I.; Singh, M.; Stiegler, H.; Gnade, B. E. & Quevedo-Lopez, M. A., (2011). Ferroelectric random access memory based on one transistor one capacitor device structure for flexible electronics, in preparation.

Merz, W. J., (1956). Switching time in ferroelectric $BaTiO_3$ and its dependence on crystal thickness, *J. Appl. Phys.,* Vol. 27, No. 8, pp. 938-943

Naber, R. C. G.; Blom, P. W. M.; Marsman, A. W. & Leeuw, D. M., (2004). Low voltage switching of a spin cast ferroelectric polymer, *Appl. Phys. Lett.,* Vol. 85, No. 11, pp. 2032-2034

Naber, R. C. G.; Tanase, C.; Blom, P. W. M.; Gelinck, G. H.; Marsman, A. W.; Touwslager, F. J.; Setayesh, S. & De leeuw, D. M., (2005). High-performance solution-processed polymer ferroelectric field-effect transistors, *Nat. Mater.,* Vol. 4, pp. 243-248

Nakajima, T.; Abe, R.; Takahashi, Y. & Furukawa, (2005). Intrinsic switching characteristics of ferroelectric ultrathin vinylidene fluoride/trifluoroethylene copolymer films revealed using Au electrode, *Jpn. J. Appl. Phys.,* Vol. 44, No. 45, pp. L 1358-L 1388

Nalwa, H. S., (1995a) *Ferroelectric polymers chemistry, physics, and applications,* Marcel Dekker, Inc, New York

Nalwa, H. S., (1995b). Ferroelectric nylons, In: *Ferroelectric polymers chemistry, physics, and applications*, Hari Singh Nalwa, pp. 63-181, Marcel Dekker, Inc., New York

Park, Y. J.; Kang, S. J; Park, C.; Kim, K. J.; Lee, H. S; Lee, M. S; Chung, U. I & Park, I. J., (2006). Irreversible extinction of ferroelectric polarization in P(VDF-TrFE) thin films upon melting and recrystallization, *Appl. Phys. Lett.,* Vol 88, p. 242908

Pauling, L. (1960). The Nature of the Chemical Bonding, (3rd edition), *Cornell University Press*, Ithaca, NY, p. 644

Reynolds, N. M.; Kim, K. J.; Chang, C. & Hsu, S. L., (1989). Spectroscopic analysis of the electric field induced structural changes in vinylidene fluoride/trifluoroethylene copolymers, *Macromolecules*, Vol. 22, No. 3, pp. 1092-1100

Salimi, A & Yousefi, A. A. (2004). Conformational changes and phase transformation mechanisms in PVDF solution-cast films, *Journal of Polymer Science Part B: Polymer Physics,* Vol. 42, No. 18, pp. 3487-3495

Stolichnov, I.; Tagantsev, A.; Setter, N.; Cross, J. S. & Tsukada, M., (2003). Crossover between nucleation-controlled kinetics and domain wall motion kinetics of polarization reversal in ferroelectric films, *Appl. Phys. Lett.,* Vol. 83, No. 16, pp. 3362-3364

Tagantsev, A. K.; Stolichnov, I.; Setter, N.; Cross, J. S. & Tsukada, M., (2002). Non-Kolmogorov-Avrami switching kinetics in ferroelectric thin films, *Phys. Rev. B,* Vol. 66, No. 21, p. 214109

Tajitsu, Y.; Ogura, H.; Chiba, A. & Furukawa, T. (1987). Investgation of switching characteristics of vinylidene fluoride/trifluoroethylene copolymers in relation to their structures, *Jpn. J. Appl. Phys.*, Vol. 26, No. 4, pp. 554-560

Tajitsu, Y., (1995). Effects of thickness on ferroelectricity in vinylidene fluoride and trifluoroethylene copolymers, *Jpn. J. Appl. Phys.,*Vol. 34, Part 1, No. 9B, pp. 5418-5423, doi: 10.1143/JJAP.34.5418

Tashiro, K., (1995). Crystal structure and phase transistion of PVDF and related copolymers, In: *Ferroelectric polymers chemistry, physics, and applications*, Hari Singh Nalwa, pp. 63-181, Marcel Dekker, Inc., New York

Xia, F.; Xu, H. S.; Fang, F.; Razavi, B.; Cheng, Z.-Y.; Lu, Y.; Xu, B. M. & Zhang, Q. M., (2001). Thickness dependence of ferroelectric polarization switching in poly(vinylidene fluoride-trifluoroethylene) spin cast films, *Appl. Phys. Lett.,* Vol. 78, No. 8, pp. 1122-1124

Xu, H. S.; Shanthi, G.; Bharti, V & Zhang, Q. M, (2000). Structure, Conformational, and Polarization Changes of Poly(vinylidene fluoride-trifluotoethylene) Copolymer induced by high-energy electron irradiation, *Macromolecules*, Vol. 33, No. 11, pp. 4125-4131, doi: 10.1021/ma9919561

Xu, H. S.; Zhong, J. H.; Liu, X. B.; Chen, J. H. & Shen, D., (2007). Ferroelectric and switching behavior of poly(vinylidene fluoride-trifluoroethylene) copolymer ultrathin films with polypyrrole interface, *Appl. Phys. Lett.,* Vol. 90, No. 9, p. 092903, doi: 10.1063/1.2710477.

Xu, H. S.; Liu, X. B.; Fang, X. R.; Xie, H. F.; Li, G. B.; Meng, X. J.; Sun, J. L. & Chu, J. H., (2009). Domain stabilization effect of interlayer on ferroelectric poly(vinylidene fluoride- trifluoroethylene) copolymer ultrathin film, *J. Appl. Phys.,* Vol. 105, No. 3, p. 034107,

Yamada, T.; Kitayama, T., (1981). Ferroelectric properties of vinlidene fluoride-trifluoroethylene copolymers, *J. Appl. Phys.,* Vol. 52, No. 11, pp. 6859-6863

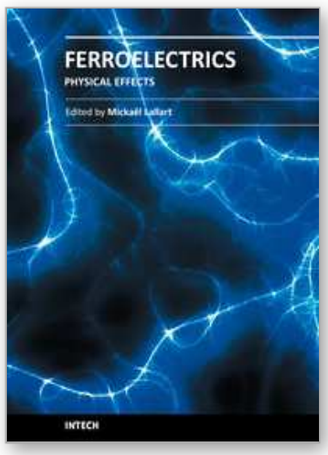


**Ferroelectrics - Physical Effects**

Edited by Dr. MickaÃ«l Lallart

ISBN 978-953-307-453-5
Hard cover, 654 pages
**Publisher** InTech
**Published online** 23, August, 2011
**Published in print edition** August, 2011

Ferroelectric materials have been and still are widely used in many applications, that have moved from sonar towards breakthrough technologies such as memories or optical devices. This book is a part of a four volume collection (covering material aspects, physical effects, characterization and modeling, and applications) and focuses on the underlying mechanisms of ferroelectric materials, including general ferroelectric effect, piezoelectricity, optical properties, and multiferroic and magnetoelectric devices. The aim of this book is to provide an up-to-date review of recent scientific findings and recent advances in the field of ferroelectric systems, allowing a deep understanding of the physical aspect of ferroelectricity.



**InTech Europe**
University Campus STeP Ri
Slavka Krautzeka 83/A
51000 Rijeka, Croatia
Phone: +385 (51) 770 447
Fax: +385 (51) 686 166
www.intechopen.com

**InTech China**
Unit 405, Office Block, Hotel Equatorial Shanghai
No.65, Yan An Road (West), Shanghai, 200040, China
中国上海市延安西路65号上海国际贵都大饭店办公楼405单元
Phone: +86-21-62489820
Fax: +86-21-62489821

IntechOpen